Dynamic DNA methylation landscape defines brown and white cell specificity during adipogenesis

CrossMark

Yen Ching Lim [1,2], Sook Yoong Chia [2], Shengnan Jin [1], Weiping Han [3], Chunming Ding [1,*], Lei Sun [2,4,**]

ABSTRACT

Objective: DNA methylation may be a stable epigenetic contributor to defining fat cell lineage.
Methods: We performed reduced representation bisulfite sequencing (RRBS) and RNA-seq to depict a genome-wide integrative view of the DNA methylome and transcriptome during brown and white adipogenesis.
Results: Our analysis demonstrated that DNA methylation is a stable epigenetic signature for brown and white cell lineage before, during, and after differentiation. We identified 31 genes whose promoters were significantly differentially methylated between white and brown adipogenesis at all three time points of differentiation. Among them, five genes belong to the Hox family; their expression levels were anti-correlated with promoter methylation, suggesting a regulatory role of DNA methylation in transcription. Blocking DNA methylation with 5-Aza-cytidine increased the expression of these genes, with the most prominent effect on *Hoxc10*, a repressor of BAT marker expression.
Conclusions: Our data suggest that DNA methylation may play an important role in lineage-specific development in adipocytes.

Keywords Brown adipogenesis; White adipogenesis; DNA methylation; Hoxc10; Next generation sequencing

1. INTRODUCTION

Sedentary life style and frequent consumption of energy-dense food are primary causes for the escalating obesity rate. Obesity is a known risk factor for type 2 diabetes, cardiovascular diseases, hyperglycaemia, dyslipidaemia, hypertension, and cancers [1—3]. As such, understanding fat biology is a key area of interest. While white adipose tissues (WAT) function mainly as a primary organ for energy storage in the form of triglycerides to provide fuels during starvation, brown adipose tissues (BAT) serves as the major organ for non-shivering thermogenesis. Brown adipocytes are densely packed with uncoupled mitochondria expressing high levels of *Ucp1* that facilitates proton leak across the inner membrane to matrix, resulting in heat generation. Recent studies have also shown the existence of a third category of fat cells, known as beige or brite adipocytes. Dispersed among white adipose tissues, these beige adipocytes look indistinguishable from white adipocytes in the basal state but take morphological resemblance to BAT and express high levels of *Ucp1* when activated by β-adrenergic receptor agonist or proliferator-activated receptor-γ (Pparγ) [4—6]. This unique feature of brown and beige adipocytes make them attractive targets for obesity therapy [5—8], which has been

further bolstered by the recent re-discovery of BAT in adult human using positron emission tomography (PET) scans [9—11].
Elucidating molecular mechanisms underlying lineage-specific development in brown and white adipocytes is a topic of great interest. Recent years have seen significant progress in understanding the transcriptional regulatory circuits in these processes [12], but our knowledge about epigenetic regulation at DNA methylation level remains very limited. DNA methylation is one of the most extensively studied epigenetic mechanisms in a variety of biological processes including cell differentiation, cell type specificity, X chromosome inactivation, genomic imprinting, and development [13,14]. Selective examination of methylation status of adipogenic markers (*Leptin*, *Pparg2*, *Fabp4* and *LPL*) and non-adipogenic makers (*MYOG*, *CD31* and *GAPDH*) in human mesenchymal stem cells, adipose tissue-derived stems cells, and embryonic stem cells showed that adipogenic promoters tend to be hypomethylated compared to non-adipogenic promoters, suggestive of an epigenetic control on the expression of adipogenic genes [15]. A previous study by Gentile et al. [16] reported that silencing *DNMT1* resulted in an acceleration of adipogenesis, which was accompanied by an apparent early induction of adipocyte-specific genes (*Glut4*, *Fabp4* and *PPAR*γ). Adiponectin, a

[1]School of Laboratory Medicine and Life Science, Wenzhou Medical University, Wenzhou, Zhejiang 325035, China [2]Cardiovascular and Metabolic Disorders Program, Duke-NUS Graduate Medical School, 8 College Road, Singapore 169857, Singapore [3]Singapore Bioimaging Consortium, Agency for Science, Technology and Research (A*STAR), Singapore 138667, Singapore [4]Institute of Molecular and Cell Biology, 61 Biopolis Drive, Proteos, Singapore 138673, Singapore

*Corresponding author.
E-mail: cmding@gmail.com (C. Ding).

**Corresponding author. Cardiovascular and Metabolic Disorders Program, Duke-NUS Graduate Medical School, 8 College Road, Singapore 169857, Singapore.
E-mail: sun.lei@duke-nus.edu.sg (L. Sun).

glucose metabolism regulator, was also found to be hypermethylated in promoter region of obese mice [17].

In this study, we seek to understand the epigenetic contribution of DNA methylation in controlling adipocyte differentiation and brown/white cell type definition. We comprehensively analyzed the DNA methylome of brown and white adipocytes during the course of differentiation. We found an overall hypermethylation in mature adipocytes compared with preadipocytes as well as in white adipocytes compared with brown adipocytes across the course of adipogenesis. Comparative analysis of brown vs. white methylome reveals differential methylation states of a set of *Hox* genes, whose mRNA levels are depot specific and likely regulated by DNA methylation.

2. RESULTS

2.1. An overview of DNA methylation profiles for three adipogenesis models

To profile the DNA methylome for lineage specific adipogenesis, we isolated primary murine brown and white pre-adipocytes from inter-scapular and inguinal depots, respectively, for *in vitro* differentiation to mature adipocytes as described in the Methods. To examine methyl-ome changes during browning and BAT activation, we also treated white adipocytes with norepinerphine (NE) for five days and acutely treated brown adipocytes with NE for 4 h to induce the expression of key BAT markers (Figure 1A). The biological validity of each model was confirmed by real-time quantitative PCR to examine the expression of the pan-adipogenic markers (*AdipoQ, Fabp4, Ppar*γ) and BAT-specific markers (*Pgc1*α*, Ucp1, Cidea*) across the differentiation stages (Figure 1B).

Each of these nine samples listed in Figure 1A was subjected to a modified reduced representation bisulfite sequencing (RRBS) pipeline developed in-house [18] to quantify DNA methylation. Using a mini-mum sequencing depth of 10 as a cut off, we obtained an average of 1.3 million autosomal CpGs per sample with a minimal conversion rate at 99.2% (Figure S1A–S1B). To facilitate comparison, only CpGs with $\geq$10 coverage in all nine samples were retained for downstream analysis. This reduced the pool of analyzable autosomal CpGs to 838,481. Similar to previous study in human placenta [19], 33%, 40% and 33% of these sites were distributed in promoters (defined as 1 kb upstream and 500 bp from TSS, 287,243 CpGs, 33%), gene bodies (defined as from end of promoter to TTS, 315,733 CpGs, 40%) and intergenic regions (27%) (Figure 1C top panel). About half of the CpGs were located within 6 kb of annotated CpG island (CGIs), comprising of CGIs (37%), CG shores (2 kb up/downstream from CGI, 10%), and CG shelves (2 kb up/downstream from CG shores, 3%) (Figure 1C bottom panel). On a regional level, 47.5% of promoters, 56.1% of gene bodies and 63.8% of CGIs are covered by at least two CpGs (Figure 1C). Out of the 838,481 CpGs, 122,818 CpGs (14.7%) were mapped to repetitive elements (Figure S1C).

To ask what biological information the DNA methylome and tran-scriptome may encode, we performed principle component analysis and hierarchical clustering to both datasets. Clustering with tran-scriptome data revealed separation of samples by their states of differentiation (Figure 1D) associated with a functional specializa-tion towards lipid metabolism (Figure S3A). However, DNA meth-ylomes grouped samples by cell types regardless their differentiation status (Figure 1E). Noteworthy, NE treatment in WAT and BAT did not change their clustering pattern based on DNA methylation. Therefore, our results demonstrated that DNA methylation signature represents a stable epigenetic mark for different cell lineages.

2.2. Overall hypermethylation during adipogenesis

To determine how the DNA methylome changes during adipogenesis, we examined DNA methylation profile changes during the time course of differentiation at single CpG and genomic region levels. First, all analyzed CpGs were categorized into lowly methylated (LM, <30%), partially methylated (PM, 30−70%) and highly methylated (HM, >70%) classes. During both white and brown adipogenesis, there was a decrease in LM CpGs and a corresponding increase of PM and HM CpGs (Figure 2A). Further assessment of methylation difference for each CpG revealed a consistent higher abundance of hyper- than hypomethylated CpGs relative to an earlier time point (Figure 2A, Figure S2A). These data suggested an overall increase in DNA methylation during both white and brown adipogenesis. Interestingly, although most of the significantly differentially methylated CpGs (DMC) (Figure 2B) were located in intronic and intergenic regions, dominance of hypermethylation was most pronounced in promoter regions (Figure 2C). Independent functional enrichment analyses on signifi-cantly differentially methylated promoters (DMP) of brown and white adipogenesis (day 0 vs day 4) showed significant enrichments in cell proliferation and differentiation (Figure S2B).

2.3. White adipocytes exhibit consistent overall hypermethylation compared to brown adipocytes during all differentiation stages

Intrigued by cell lineage specificity of the DNA methylome from Figure 1F, we proceeded to investigate the systematic differences between BAT and WAT throughout adipogenesis. Time-matched comparisons between BAT and WAT revealed hypermethylated CpGs significantly outnumbered hypomethylated CpGs (p < 0.05, binomial test, Figure 2D,E). Similar to findings from adipogenesis time course analysis, significantly differentially methylated CpGs (DMCs) (Figure 2F) were mostly located in intronic or intergenic regions. However, unlike in adipogenesis time course analysis, dominance of hypomethylated DMCs (with respect to WAT) was found in exonic regions instead of promoters (Figure 2F). In addition, significantly differentially methyl-ated promoters (DMPs) between mature BAT and WAT showed enrichment for networks related to brown fat functions (Figure S2C).

2.4. General anti-correlation between promoter methylation and gene expression

To investigate if changes in promoter DNA methylation were associ-ated with gene expression changes, we used transcriptome data ob-tained from sample-matched RNA-seq data. Global gene ontology analyses on the regulated genes during white and brown adipogenesis showed significant enrichments in mitochondrial respiratory chain and lipid metabolic process terms respectively (Figure S3A), whereas top up-regulated GO in mature BAT relative to mature WAT includes mitochondrial respiratory chain and fatty acid oxidation (Figure S3B). This clearly demonstrated that our RNA-seq data accurately reflects biological changes during differentiation and between different cell types. An overall negative correlation between promoter methylation and gene expression was observed when comparing WAT and BAT types (Figure S4A) and cells at different time course of adipogenesis (Figure S4B).
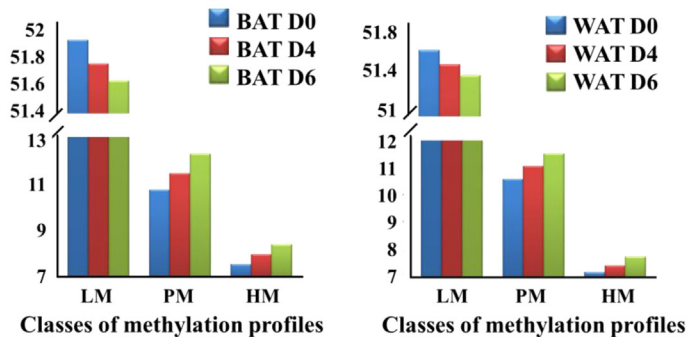
2.5. Hox family genes were consistently differentially methylated between brown and white adipogenesis at all time points

We identified 31 genes with significant changes in DNA methylation when comparing BAT vs. WAT at all three time points during adipo-genesis (Figure 3A). Out of these 31 genes (Figure 3B), 23 and 8 were hyper- and hypomethylated, respectively, in WAT compared to BAT. There was a significant enrichment of an important class of
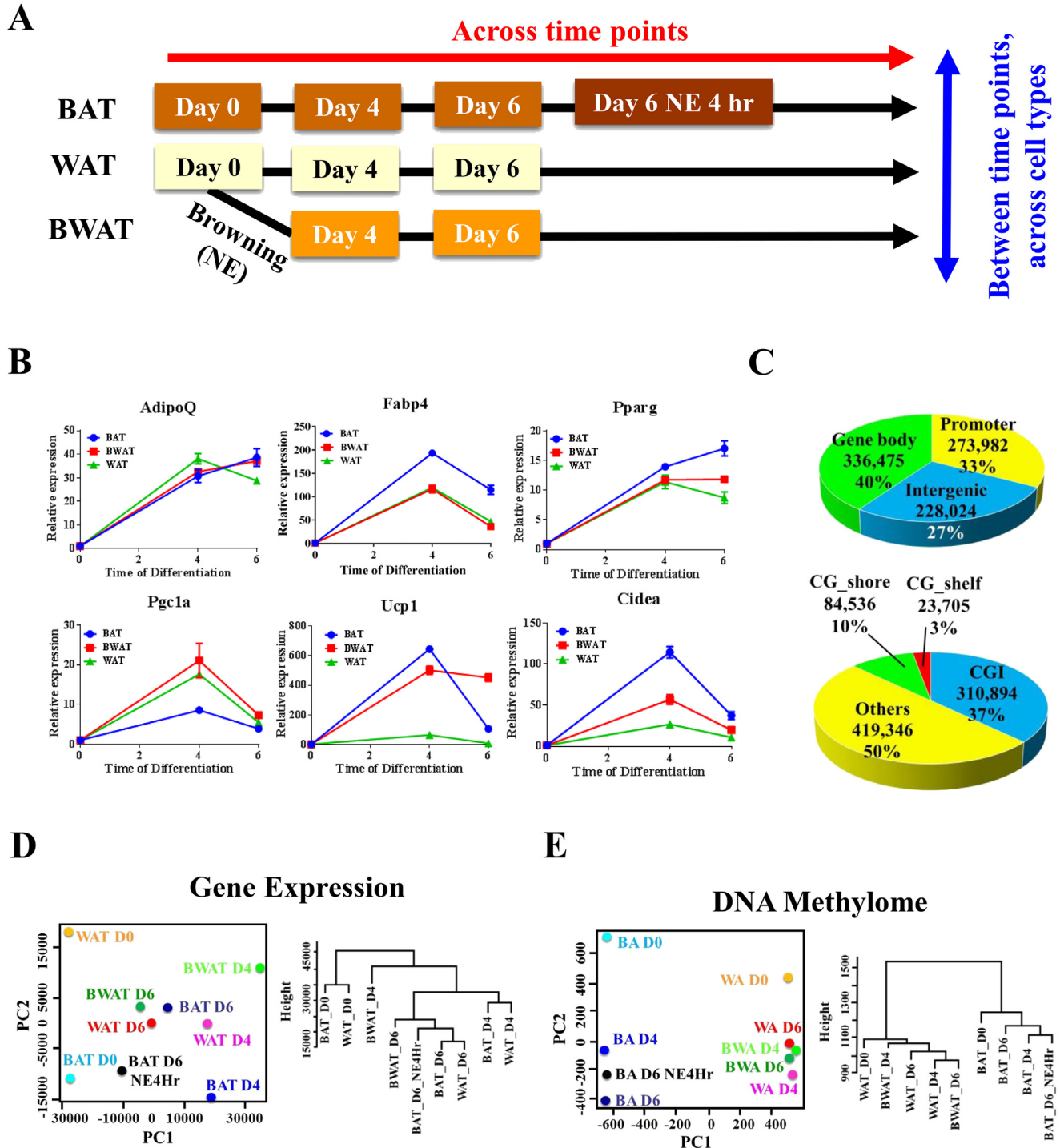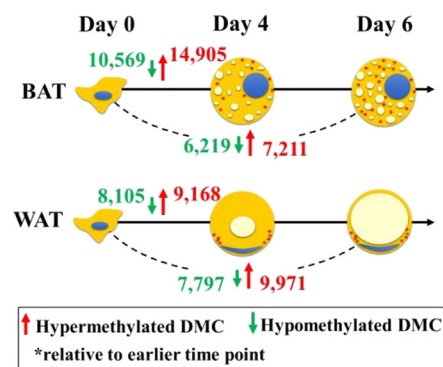
Figure 1: Data overview. (A) Study Design. BA: Brown adipocytes, WA: white adipocytes, BWA: brown induced white adipocytes. (B) Real-time quantitative PCR analyses of gene expression profiles for general adipogenic markers (top panel: AdipoQ, Fabp4 and Pparγ) and brown fat specific markers (bottom panel: Pgc1α, Ucp1 and Cidea) during brown, white, and brown-induced adipogenesis. Error bars represent mean ± SEM, n = 3. BAT: brown adipocytes, WAT: white adipocytes, BWAT: brown induced white adipocytes. (C) A total of 838,481 autosomal CpGs with sequencing depth of ≥10 for all nine samples were included in all downstream analyses. Covered CpGs were approximately uniformly distributed in promoters, gene bodies, and intergenic regions. 50% of the CpGs were located within 6 kb from annotated CGIs (CGI, CG shelf and CG shore). (D) PCA and hierarchical clustering analyses of all nine analyzed samples using gene expression from RNA-seq separated samples by states of differentiation. (E) PCA and hierarchical clustering analyses of all nine analyzed samples using DNA methylation separated samples by cell types. Average DNA methylation percentage generated by merging nearby CpGs of less than 500 bp was used.
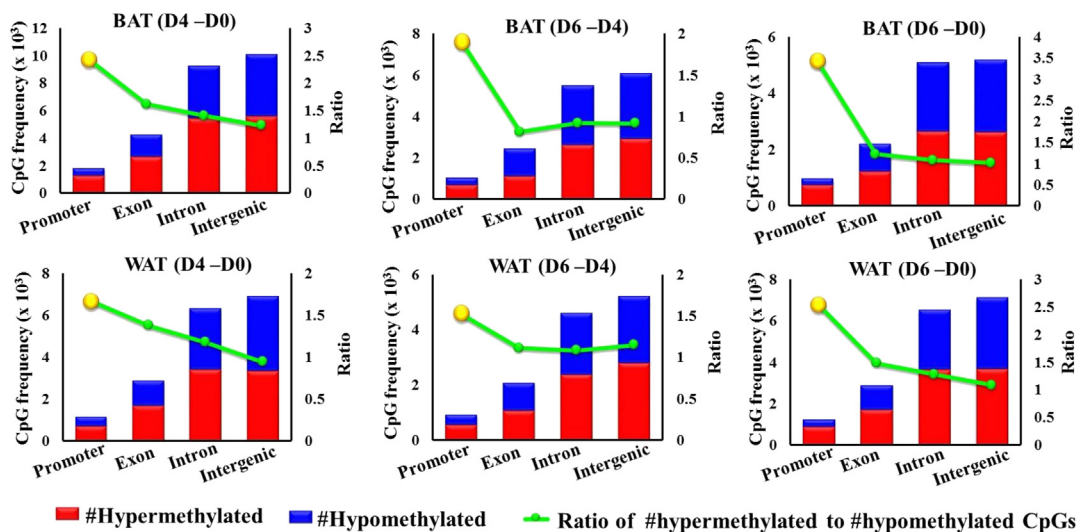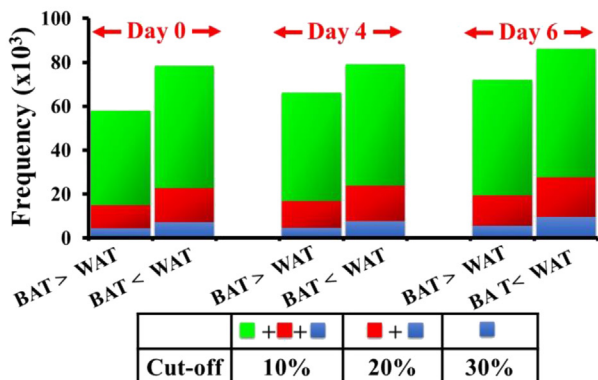
A

B

C

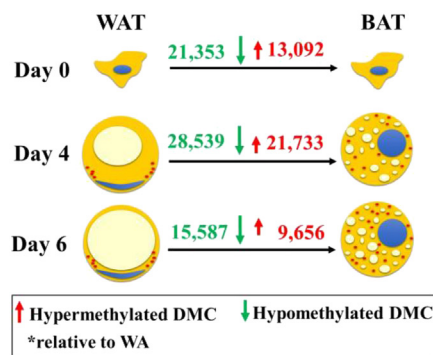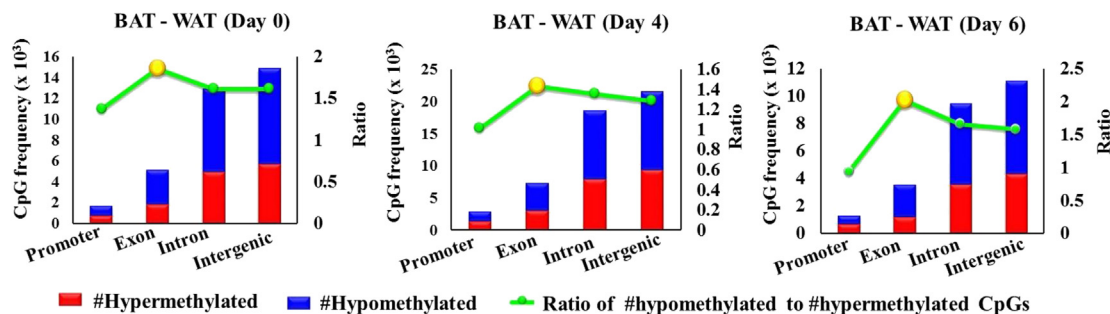#Hypermethylated #Hypomethylated Ratio of #hypermethylated to #hypomethylated CpGs

D

E

↑ Hypermethylated DMC ↓ Hypomethylated DMC
*relative to WA

F

#Hypermethylated #Hypomethylated Ratio of #hypomethylated to #hypermethylated CpGs

transcription factors, Hox family genes, including *Hoxa2*, *Hoxa5*, *Hoxc4*, *Hoxc9* and *Hoxc10* (p < 0.01, hypergeometric test). Hox gene members are a super family of transcription factors [20], which are highly conservative in sequence and functions. Recent work has demonstrated the involvement of Hox genes in the adipogenic field such as cell specific expression and involvement in metabolic diseases such as diabetes [20,21]. For instance, *Hoxc9*, hypermethylated in BAT, is a well-established white fat marker [22] (Figure 3B). *Hoxc8* was highly expressed in human WAT progenitor cells to repress brown fat markers [23].

Interestingly, for all these five *Hox* genes, gene expression by RNA-seq inversely correlates with the methylation pattern. *Hoxa2*, *Hoxa5* and *Hoxc4* were enriched in BAT, consistent with their hyper-methylation, while the expression of *Hoxc9* and *Hoxc10* was lower in BAT, consistent with their hypo-methylation. Furthermore, the relative expressions of these genes were confirmed by q-PCR. *Hoxa2*, *Hoxa5*, *Hoxc9* and *Hoxc10* showed consistent anti-correlation between methylation and gene expression changes (Figure 3C, right panel). Additionally, we analyzed the relative expressions of these *Hox* genes in mice tissue samples and observed a similar pattern as the *in vitro* model (Figure 3D).

To test whether the expression pattern of these genes is conserved between mouse and human, we examined RNA-seq data obtained from human adult subcutaneous and fetal brown adipose fats (Figure 3E). Consistent with both mouse *in vitro* and *in vivo* models, *Hoxc9* and *Hoxc10* exhibited tissue specific expression in human.

2.6. Inhibition of DNA methylation in Hox gene promoters by 5-Aza-cytidine treatment up regulates gene expression

Next, we asked if there is a potential causative relationship between promoter DNA methylation and gene expression for the *Hox* genes. We induced both white and brown pre-adipocytes to differentiate for five days in the presence of 5-Aza-cytidine, a blocker of methylation. Upon 5-Aza-induced demethylation, *Hoxa2* and *Hoxa5* were significantly upregulated in WAT, where their promoters were hypermethylated, but not in BAT, where their promoters were lowly methylated. *Hoxc9* and *Hoxc10* were up regulated more in BAT than in WAT, probably due to their hyper-methylation in BAT (Figure 4A). Hoxc10 was of particular interest and chosen for further analysis, because it manifested the most significant change in expression upon de-methylation, and our recent data have demonstrated that it is a repressor for BAT marker expression in WAT, which will be reported in a separate study.

Because 5-Aza treatment causes global demethylation, it is possible the observed changes in gene expression are due to an indirect effect. To exclude this possibility, we treated preadipocytes with 5-Aza for 3 days without adding the differentiation cocktail (Figure 4B), and, in a separate experiment, treated the differentiated mature brown adipocytes (D5) (Figure 4C) with 5-Aza for three days. Up-regulation of *Hoxc10* was detected in both cases, which argues that the up

regulation of *Hoxc10* by demethylation is likely to be a causative effect and independent of the differentiation process.

To provide a precise picture of the methylation status in *Hoxc10* promoter at individual CpG level, we performed bisulfite conversion and cloned *Hoxc10* promoter region for sequencing (Figure 4D). Consistently with our high throughout sequencing data, methylation was only found in BAT but not WAT. Upon 5-Aza treatment, more than 60% of the CpG sites were unmethylated (Figure 4E), which was accompanied by an up-regulation of *Hoxc10* expression (Figure 4A—C). Taken together, our study demonstrated that BAT-specific methylation of *Hoxc10* promoter contributes to its tissue-specific gene expression repression.

3. DISCUSSION

As one of the most well-studied epigenetic mechanisms, DNA methylation has been shown to be important in regulating cell differentiation [15,24] and for defining cell lineages. Here, we present the first comprehensive and dynamic genome-wide DNA methylation landscape for both white and brown adipogenesis processes, to understand how fat cells differentiation and cell fate commitment are regulated by DNA methylation.

While gene expression profiles represent the dynamic status during cell differentiation in both BAT and WAT adipogenic models, DNA methylation profiles are consistently reflective of cell lineages. This suggests that while DNA methylation is known to regulate gene expression, its function may be better appreciated in development. Surprisingly, only 31 genes were consistently differentially methylated between BAT and WAT in the entire differentiation process. Five out of these 31 genes are *Hox* family genes that encode transcription factors that bind to DNA enhancers via homeodomain to either activate or suppress gene expression. We observed a similar differential expression pattern for *Hoxc10* in mouse primary cell lines and tissues as well as in human tissues. We also demonstrated that promoter methylation may have a direct effect in regulating *Hoxc10* expression. Among many essential roles of the Hox genes include proper embryo development and control of cell death and cell proliferation [20,25]. A recent study by Benton et al. [26] compared methylation changes before and after gastric bypass and weight loss human subcutaneous adipose and found significant methylation changes in *Hox* genes from multiple *Hox* clusters, suggesting the change in methylation of *Hoxc10* is clinically relevant. Collectively, our work suggests a potential pathway for how DNA methylation regulates adipogenesis via cell lineage commitment. This serves as an important and solid basis for supporting the role of DNA methylation being a stable epigenetic signature in defining brown and brown adipocyte lineage.

One limitation of our study is that brown and white preadipocytes were isolated from different fat depots. We can't preclude the possibility that the observed methylation difference between BAT and WAT might be

Figure 2: Overall hypermethylation during adipogenesis and hypermethylation in white adipocytes than brown adipocytes. (A) Individual CpGs grouped by methylation levels into LM (<30%), PM (30—70%) and HM (>70%) during brown (left panel) and white (right panel) adipogenesis. (B) Frequency of DMCs during brown and white adipogenesis. Comparisons were made relative to the earlier time point (i.e. day 4 — day 0, day 6 — day 0). Green arrow: hypomethylation. Red arrow: hypermethylation. (C) Proportions of significantly differentially methylated CpGs in each genomic category. DMCs were mostly located in intron and intergenic regions. Ratio between hyper- and hypomethylated DMCs given by line plot. (D) Frequencies of hyper- and hypomethylated CpGs between BAT and WAT at various days of differentiation (day 0, 4 and 6), using varying cutoffs of 10%, 20%, and 30%. (E) Frequency of DMCs during with respect to WAT at days 0, 4, and 6. Green arrow: hypomethylation. Red arrow: hypermethylation. (F) Proportions of significant differentially methylated CpGs in each genomic category. DMCs were mostly located in intron and intergenic regions. Ratio between hyper- and hypomethylated DMCs given by line plot.
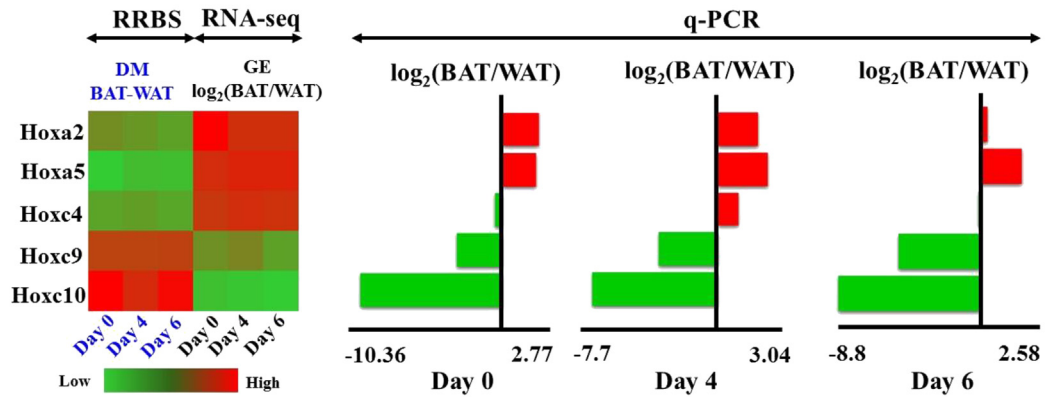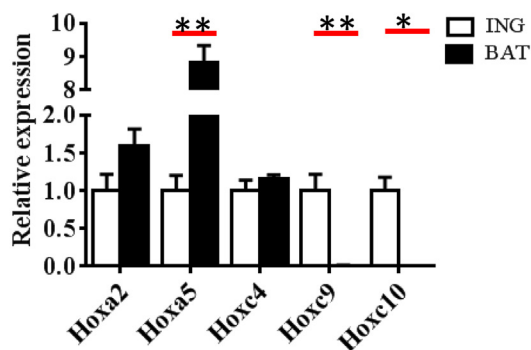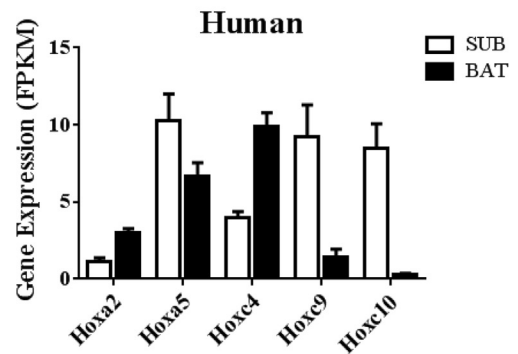
A
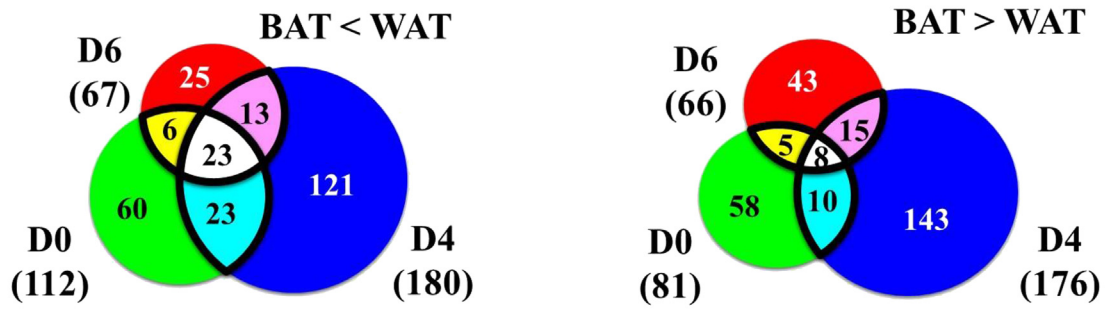
B
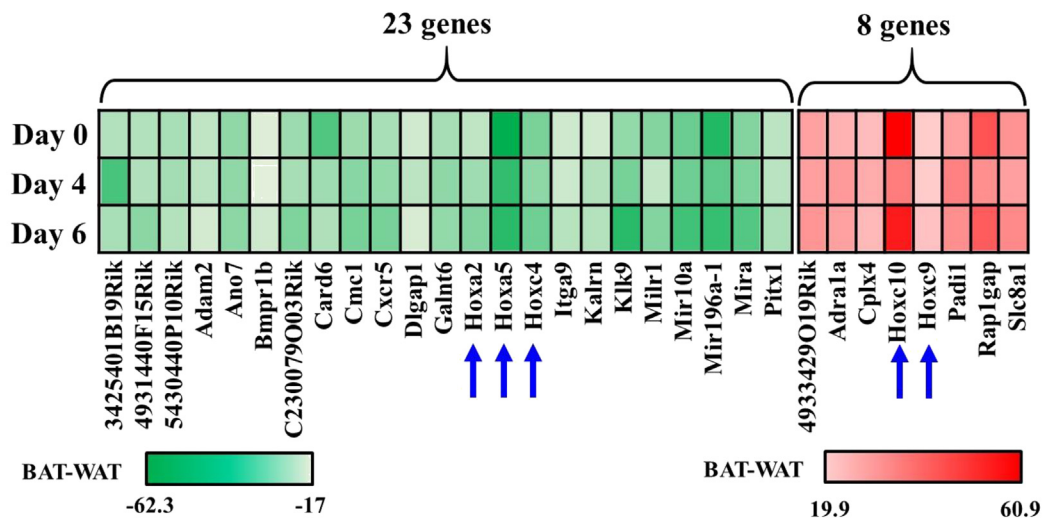
C

D

E

related to their distinct localization. Studies to compare interscapular WAT covering BAT with BAT should be explored in the future.

4. EXPERIMENTAL PROCEDURES

4.1. Cell isolation and cell culture
Brown and white preadipocytes were isolated from interscapular brown adipose tissues and inguinal white fat depots respectively. Eight BL6 mice were sacrificed at three weeks and the harvested fat tissues were minced, collagenase digested, and fractionated. Pre-adipocytes, which were enriched at the bottom stromal vascular fractions, were collected, resuspended, and cultured to confluence. Subsequently, white and brown pre-adipocytes were induced to differentiate into mature brown and white adipocytes by exposure to differentiation medium: 10% (v/v) FBS DMEM, 850 nM insulin (Sigma), 0.5 μM dexamethasone (Sigma), 250 μM 3-isobutyl-1-methylxanthine (Sigma), and 1 μm Rosiglitazone (Sigma). 48 h later, we replaced the induction medium with maintenance medium (10% FBS, DMEM). In addition, an independent set of white pre-adipocytes was induced to differentiation in the presence of norepinephrine (1uM). Cells were harvested at days 0, 4 and 6 for both RRBS and RNA-seq library preparation.

4.2. Reduced representation bisulfite sequencing
A total of nine samples were included in the study. Experimental and computational procedures followed previously described methods [18,19] with some modifications. Briefly, 1 μg of genomic DNA from each sample was digested using MspI (New England Biolabs, USA) and Taq$^{\alpha}$I (New England Biolabs). The digested product was subsequently purified with the QIAquick PCR Purification Kit (QIAGEN GmbH), end-repaired, 3′-end-adenylated, and adapter-ligated using TruSeq ChIP-Seq Sample Preparation Kit (Illumina, USA). Ten microliters of the RNA adapter index adapter oligonucleotides and 3 μL of ligation mix were used in a 45 μL reaction system and the ligation was performed for 10 min at 30 °C in the adapter-ligation step. Fragments with 210—290 bp size were selected by gel electrophoresis, purified, and bisulfite treated using EZ DNA Methylation-Gold Kit (Zymo Research, USA). The bisulfite converted DNA was then PCR amplified, purified by by Agencourt AMPure XP Beads (Beckman Coulter Inc.) and validated using Agilent 2100 Bioanalyzer (Agilent Technologies, Santa Clara, CA, USA). Libraries were pooled together and analyzed by paired-end sequencing (2 × 75 bp) read on Illumina Hiseq (High Output Mode). The mouse July 2007 (NCBI37/mm9) genome assembly was used throughout the study. Sequencing data were deposited into the GEO database with accession number GSE80961.

4.3. Differential DNA methylation analysis
Differential methylation analysis was performed at both the single CpG and regional levels. Only autosome CpGs (sequencing depth ≥10) common to all nine samples were included in all subsequent analyses. Between a pair of samples, only CpGs having a methylation difference of at least 10% were selected for 2-sided fisher exact test. P values were then adjusted by the Benjamini Hochberg method. A CpG was considered significant if (i) the difference between the sample pair was at least 10%, and (ii) the FDR corrected p value < 0.05. A promoter was considered significantly differentially methylated if it contained at least two significant CpGs, both of which must be regulated in the same direction (either all hypermethylated or hypomethylated). All statistical analyses were performed using R package.

4.4. RNA-seq
Total RNAs from adipocytes were extracted according to Qiagen miRNeasy kit. RNA-seq libraries were prepared according to NEBNext Ultra Directional RNA Library Prep Kit for Illumina and ran on Hiseq2000 sequencer platform. The 100 bp paired-end reads were first quality checked with FastQC (http://www.bioinformatics.babraham.ac.uk/projects/fastqc/), subsequently aligned to mm9, using Tophat (version tophat-2.0.11). The aligned reads were then put into Cufflinks (Version 2.1.1) to quantify gene expression into units known as fragments per kilobase of exon per million fragments mapped (FPKM). Genes with low expression (FPKM < 1 in all samples) were removed, leaving 14,491 autosomal genes. Sequencing data were deposited into the GEO database with accession number GSE80961.

4.5. q-PCR
RNA was reverse transcribed into cDNA with random primers (SuperScript II Reverse Transcriptase, Invitrogen), followed by PCR amplification using gene specific primers. Sybr Green based qPCR was performed in an Applied Biosystems 7900HT Fast Real-time PCR System, using RPL23 as an internal control for normalization. Data were analyzed by the relative quantification ($\Delta\Delta C_t$) method.
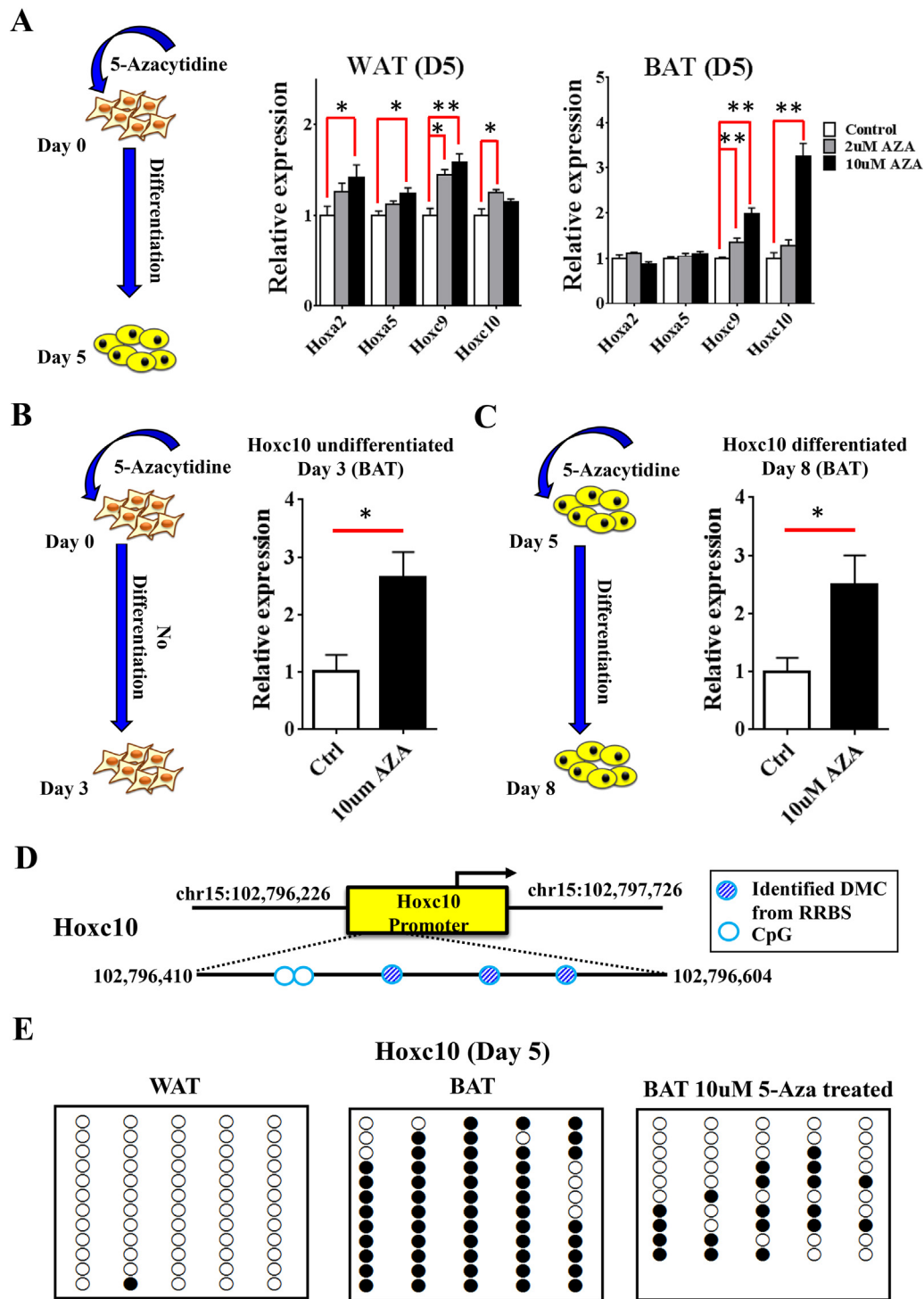
4.6. 5-Aza-cytidine drug treatment
5-Aza-cytidine treatment was administered to brown and white adipocytes under three different conditions. (i) Confluent preadipocytes were induced to differentiate, and differentiating cells were incubated with 0, 2 μM and 10 μM 5-Aza-cytidine for five days. (ii) Confluent brown preadipocytes were treated with 0 μM and 10 μM 5-Aza-cytidine for three days without differentiation induction. (iii) Differentiated brown adipocytes (day 5) were treated with 0 μM and 10 μM 5-Aza-cytidine for three days.

4.7. Cloning and bisulfite sequencing
Total genomic DNA was isolated using QIAamp DNA Micro Kit (Qiagen). Bisulfite conversion was performed with 1 μg of the genomic DNA using EZ DNA Methylation-Gold Kit (Zymo Research), according to manufacturer's instructions. Bisulfite converted DNA was then amplified in the Hoxc10 promoter region using the following set of primers: forward, TTAAAAGTAAGTTGAAGTTTTTGTTTTTTTGTTTTT; reverse CCTCCTTTACCCAAAATCCCTTAAATA (Table S1). The PCR

Figure 3: Promoter methylation differences for five Hox genes were associated with gene expression differences between white and brown adipocytes during adipogenesis. (A) Frequencies of overlapping DMPs between BAT and WAT at days 0, 4, and 6. DMPs were split into BAT > WAT and BAT < WAT. (B) Heatmap representation of methylation differences for gene promoters (between BAT and WAT) which were either consistently hypo or hypermethylated from day 0—6 of cell differentiation. Five *Hox* genes have been indicated by blue arrows. (C) Promoter DNA methylation difference (RRBS) with corresponding gene expression (RNA-seq) difference between WAT and BAT at days 0, 4, and 6 for five selected *Hox* genes (*Hoxa2, Hoxa5, Hoxc4, Hoxc9, and Hoxc10*). Gene expression difference for five selected *Hox* genes were validated with q-PCR results. (D) Expression of the five *Hox* genes in mouse inguinal and brown tissues. Error bars represent mean ± SEM, n = 4. *p ≤ 0.05, **p ≤ 0.01. (E) RNA-seq expression of the five *Hox* genes in human subcutaneous and brown tissues. Error bars represent mean ± SEM, n = 3/4.

Figure 4: Inhibition of DNA methylation in Hox gene promoters by 5 Aza-cytidine treatment alters gene expression. (A) Schematic diagram of 5-Aza-cytidine treatment to BAT and WAT pre-adipocytes (left panel). Expression of Hox genes subjected to 2 μm and 10 μm of 5-Aza-cytidine treatment in BAT middle panel) and WAT (right panel) at day 5. There was a prominent elevation of *Hoxc10* gene expression in BAT brought by 10 μm 5-Aza. n = 4. (B—C) Brown pre-adipocytes were treated with 10 μm 5-Aza-cytidine and expression of Hoxc10 investigated under different differentiation conditions. (B) Undifferentiated BAT at day 3. (C) Cells treated at day 5 and harvested at day 8. Cells induced to differentiate and harvested at day 8. n = 3/4. (D) Selected *Hoxc10* promoter region for further analysis. This region spans 195bp, covering five CpG sites. Striped blue circles: CpG with significant methylation difference identified from RRBS. Open blue circles: CpG not covered in RRBS study. (E) Bisulfite treatment, cloning, and sequencing performed on white (WAT) and brown (BAT) adipocytes at day 5 in *Hoxc10* promoter confirmed hypermethylation status in BAT (relative to WAT). Bisulfite sequencing of the CpG sites before (BAT) and after 5-Aza-cytidine treatment (BAT 10 μm 5-Aza treated). Each open circle represents unmethylated cytosine and closed circle represents methylated cytosine. *p ≤ 0.05, **p ≤ 0.01.

products were then TA-cloned into pGEM-T Easy vector (Promega, Madison, WI, USA), and positive clones with inserts were sequenced.

4.8. Availability of data and material

Sequencing data for DNA methylation and RNA-seq are submitted into the GEO database with accession number GSE80961.

AUTHOR CONTRIBUTIONS

C.D. and L.S. and W.H. conceived and designed the experiment. S.Y.C. and S.J. performed the experiments. Y.C.L. performed the bioinformatics analysis. C.D., L.S., and Y.C.L. wrote the manuscript.

CONFLICTS OF INTEREST

The authors declare no conflicts of interest.

APPENDIX A. SUPPLEMENTARY DATA

Supplementary data related to this article can be found at http://dx.doi.org/10.1016/j.molmet.2016.08.006.

REFERENCES

[1] Cai, L., Lubitz, J., Flegal, K.M., Pamuk, E.R., 2010. The predicted effects of chronic obesity in middle age on medicare costs and mortality. Medical Care 48:510—517.

[2] Hammond, R.A., Levine, R., 2010. The economic impact of obesity in the United States. Diabetes, Metabolic Syndrome and Obesity: Targets and Therapy 3:285—295.

[3] Olshansky, S.J., Passaro, D.J., Hershow, R.C., Layden, J., Carnes, B.A., Brody, J., et al., 2005. A potential decline in life expectancy in the United States in the 21st century. The New England Journal of Medicine 352:1138—1145.

[4] Lee, Y.H., Mottillo, E.P., Granneman, J.G., 2014. Adipose tissue plasticity from WAT to BAT and in between. Biochimica et Biophysica Acta 1842:358—369.

[5] Kajimura, S., Spiegelman, B.M., Seale, P., 2015. Brown and beige fat: physiological roles beyond heat generation. Cell Metabolism 22:546—559.

[6] Rosen, E.D., Spiegelman, B.M., 2014. What we talk about when we talk about fat. Cell 156:20—44.

[7] Giralt, M., Villarroya, F., 2013. White, brown, beige/brite: different adipose cells for different functions? Endocrinology 154:2992—3000.

[8] Harms, M., Seale, P., 2013. Brown and beige fat: development, function and therapeutic potential. Nature Medicine 19:1252—1263.

[9] Cypess, A.M., Lehman, S., Williams, G., Tal, I., Rodman, D., Goldfine, A.B., et al., 2009. Identification and importance of brown adipose tissue in adult humans. The New England Journal of Medicine 360:1509—1517.

[10] van Marken Lichtenbelt, W.D., Vanhommerig, J.W., Smulders, N.M., Drossaerts, J.M., Kemerink, G.J., Bouvy, N.D., et al., 2009. Cold-activated brown adipose tissue in healthy men. The New England Journal of Medicine 360:1500—1508.

[11] Virtanen, K.A., Lidell, M.E., Orava, J., Heglind, M., Westergren, R., Niemi, T., et al., 2009. Functional brown adipose tissue in healthy adults. The New England Journal of Medicine 360:1518—1525.

[12] Seale, P., 2015. Transcriptional regulatory circuits controlling brown fat development and activation. Diabetes 64:2369—2375.

[13] Jaenisch, R., Bird, A., 2003. Epigenetic regulation of gene expression: how the genome integrates intrinsic and environmental signals. Nature Genetics(33 Suppl.):245—254.

[14] Jones, P.A., 2012. Functions of DNA methylation: islands, start sites, gene bodies and beyond. Nature Reviews Genetics 13:484—492.

[15] Noer, A., Sorensen, A.L., Boquest, A.C., Collas, P., 2006. Stable CpG hypomethylation of adipogenic promoters in freshly isolated, cultured, and differentiated mesenchymal stem cells from adipose tissue. Molecular Biology of the Cell 17:3543—3556.

[16] Londono Gentile, T., Lu, C., Lodato, P.M., Tse, S., Olejniczak, S.H., Witze, E.S., et al., 2013. DNMT1 is regulated by ATP-citrate lyase and maintains methylation patterns during adipocyte differentiation. Molecular and Cellular Biology 33:3864—3878.

[17] Kim, A.Y., Park, Y.J., Pan, X., Shin, K.C., Kwak, S.H., Bassas, A.F., et al., 2015. Obesity-induced DNA hypermethylation of the adiponectin gene mediates insulin resistance. Nature Communications 6:7585.

[18] Lee, Y.K., Jin, S., Duan, S., Lim, Y.C., Ng, D.P., Lin, X.M., et al., 2014. Improved reduced representation bisulfite sequencing for epigenomic profiling of clinical samples. Biological Procedures Online 16:1.

[19] Jin, S., Lee, Y.K., Lim, Y.C., Zheng, Z., Lin, X.M., Ng, D.P., et al., 2013. Global DNA hypermethylation in down syndrome placenta. PLoS Genetics 9: e1003515.

[20] Procino, A., Cillo, C., 2013. The HOX genes network in metabolic diseases. Cell Biology International 37:1145—1148.

[21] He, D., Wang, J., Gao, Y., Zhang, Y., 2011. Differentiation of PDX1 gene-modified human umbilical cord mesenchymal stem cells into insulin-producing cells in vitro. International Journal of Molecular Medicine 28: 1019—1024.

[22] Scheele, C., Larsen, T.J., Nielsen, S., 2014. Novel nuances of human brown fat. Adipocyte 3:54—57.

[23] Mori, M., Nakagami, H., Rodriguez-Araujo, G., Nimura, K., Kaneda, Y., 2012. Essential role for miR-196a in brown adipogenesis of white fat progenitor cells. PLoS Biology 10:e1001314.

[24] Kulis, M., Merkel, A., Heath, S., Queiros, A.C., Schuyler, R.P., Castellano, G., et al., 2015. Whole-genome fingerprint of the DNA methylome during human B cell differentiation. Nature Genetics.

[25] Foronda, D., de Navas, L.F., Garaulet, D.L., Sanchez-Herrero, E., 2009. Function and specificity of Hox genes. The International Journal of Developmental Biology 53:1404—1419.

[26] Benton, M.C., Johnstone, A., Eccles, D., Harmon, B., Hayes, M.T., Lea, R.A., et al., 2015. An analysis of DNA methylation in human adipose tissue reveals differential modification of obesity genes before and after gastric bypass and weight loss. Genome Biology 16:8.